

Functional Strain-Line Pattern in the Human Left Ventricle

Gianni Pedrizzetti,^{1,2} Elisabeth Kraigher-Krainer,³ Alessio De Luca,⁴ Giuseppe Caracciolo,² Jan O. Mangual,⁵ Amil Shah,³ Loira Toncelli,⁴ Federico Domenichini,⁵ Giovanni Tonti,⁶ Giorgio Galanti,⁴ Partho P. Sengupta,² Jagat Narula,² and Scott Solomon³

¹*Dipartimento Ingegneria e Architettura, Università di Trieste, Italy*

²*Department of Cardiology, Mount Sinai School of Medicine, New York, New York, USA*

³*Department of Cardiovascular Medicine, Brigham and Women's Hospital, Boston, Massachusetts, USA*

⁴*Sport Medicine Center, University of Firenze, Italy*

⁵*Dipartimento Ingegneria Civile e Ambientale, Università di Firenze, Italy*

⁶*Dipartimento Cardiologia, Ospedale SS. Annunziata, Sulmona, AQ, Italy*

(Received 24 April 2012; published 26 July 2012)

Analysis of deformations in terms of principal directions appears well suited for biological tissues that present an underlying anatomical structure of fiber arrangement. We applied this concept here to study deformation of the beating heart *in vivo* analyzing 30 subjects that underwent accurate three-dimensional echocardiographic recording of the left ventricle. Results show that strain develops predominantly along the principal direction with a much smaller transversal strain, indicating an underlying anisotropic, one-dimensional contractile activity. The strain-line pattern closely resembles the helical anatomical structure of the heart muscle. These findings demonstrate that cardiac contraction occurs along spatially variable paths and suggest a potential clinical significance of the principal strain concept for the assessment of mechanical cardiac function. The same concept can help in characterizing the relation between functional and anatomical properties of biological tissues, as well as fiber-reinforced engineered materials.

DOI: [10.1103/PhysRevLett.109.048103](https://doi.org/10.1103/PhysRevLett.109.048103)

PACS numbers: 87.19.Hh, 46.70.Lk, 47.32.C-, 87.57.N-

The analysis of continuum mechanics in terms of principal stress or principal strain has a long history, starting with the exemplary case of structural engineering, where it permits us to detect and reinforce the directions along which highest stresses develop [1]. The principal stress analysis appears particularly applicable to study fiber-reinforced materials where the structure itself presents a predefined directional pattern although the principal directions of stress do not necessarily coincide with the fibers' arrangements because of the interaction between neighboring layers [2]. The directional arrangement of stress and strain is of particular interest for natural or engineered biological tissues to identify the relation between the specific underlying anisotropic anatomical structure and the pattern along which deformation occurs or stress propagates [3,4].

The left ventricle (LV), whose cyclic contractions (about 10^5 times a day, every day) eject blood into the primary circulation, represents the fundamental life-sustaining mechanical element of the human heart. The LV cavity is shaped roughly like a prolate ellipsoid truncated at the base; of particular interest is the arrangement of the surrounding muscular tissue whose fibers bundle follows a helical path descending from the base to wrap around the apex and returning to the base after a crossover [5]. A schematic sketch of the LV geometry and fibers' pattern is reconstructed in Fig. 1 on the basis of literature (see, for example, [5,6] and references therein). Although details vary between individuals and with diseases, building a realistic atlas of the normal cardiac fiber architecture is a

current ongoing research topic [7]. This unique anatomical arrangement of cardiac fibers along a swirling path is reflected by the mechanical function of the LV [6]. Indeed, the assessment of LV deformation (strain analysis) is one important method of mechanical cardiac assessment; nevertheless the understanding of the LV tensorial contractile organization and of its relation with the underlying anatomical structures is still largely incomplete [8,9].

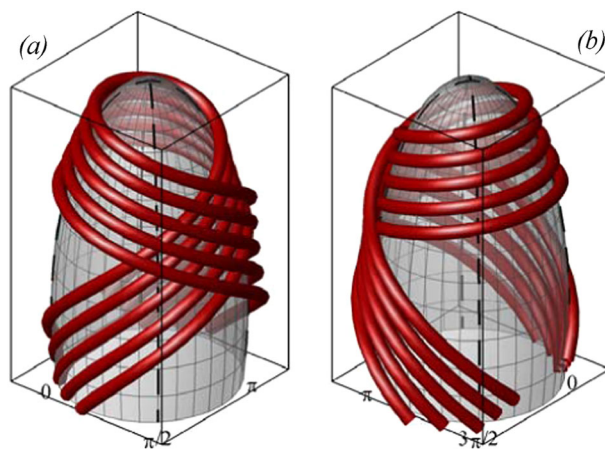


FIG. 1 (color online). Sketch of the anatomical distribution of contractile fibers in the LV, (a) and (b) correspond to two perspectives. The LV is reported upside down for visualization purpose. For anatomical reference, the value $\theta = 0$ corresponds to the position of the aortic outflow, and the right ventricle extends on the outside from there to about $\theta = \pi/2$.

Medical imaging technology (echocardiography and cardiac magnetic resonance, *in primis*) allows us, to some extent, to follow the motion of the beating tissue *in vivo*. From this, the LV tissue deformation during the contraction period (systole) can be evaluated, with the integrated strain at the end of contraction, the *end-systolic strain*, taken as a measure of LV contraction. Clinical studies typically focus on either longitudinal strain (base-to-apex shortening) or circumferential strain (reduction of transversal size) and have revealed that sometimes they are different responders to different pathologies [8]. However, the longitudinal and circumferential directions do not directly correspond to the actual fiber architecture and may be inadequate to reveal the effective contractile properties of the cardiac muscle. Very few studies have analyzed cardiac deformation employing a coordinate-free approach. Following the seminal work by Moore *et al.* [10], the three-dimensional strain components were recently measured *in vivo* with good resolution on five healthy volunteers [11]. That work was mostly aimed to evaluate strain derived from the magnetic resonance methodology; however, it demonstrated a relation between shear, principal strain direction, and LV torsion resulting from the fibers' helical structure. A more physical study, focused on the relation between the anatomy of the helical muscular band and LV motion, is reported in [12]. There, the tissue displacement (not the deformation) obtained from magnetic resonance in three healthy volunteers is analyzed by establishing a threshold for the displacements and following them in time during the systolic contraction; results show that higher displacements appear to develop along a macrostructure in the form of the helical band that witnesses a relation between form and function of the LV as a whole.

The purpose of this Letter is to further clarify the *functional* pattern along which deformation occurs in the LV. For this, we apply the principal strain analysis to assess LV systolic contraction and to characterize deformation patterns of the three-dimensional (3D) surface bounding the LV cavity in a number of normal subjects, with the objective to juxtapose the anatomical structure of the heart with its functional properties. The analysis is performed by 3D echocardiography; this technique is much more accessible than high-resolution magnetic resonance that earlier researchers used. The choice of focusing on the inner layer of the muscular tissue (the subendocardium), rather than on the entire myocardium, is dictated by the resolution of 3D images that limits the possibility of effectively differentiating figures across the thickness as it solely consists of a few pixels. Moreover, the available technology allows a more reliable analysis at the internal level (because of the tissue-cavity interface), and fibers have a less clear alignment moving toward the external side of the myocardium. Additionally, to create flow the heart muscle works by reducing the size of the blood pool boundary [13–15]; therefore, we believe that such part of the myocardial tissue represents the central element in the pump function.

Finally, starting with the simpler analysis of a two-dimensional (2D) surface permits avoiding the complexity of dealing with a 3D object from the beginning.

A group of 15 healthy volunteers (9 + 6 from two separate institutions) who were free from any cardiovascular disease or risk factor, and another series of 15 young (not professional) athletes (18–30 years old, training 2 or 3 days a week, at least 2 hours per day) underwent a 3D echocardiographic examination of the LV. The imaging data sets were then analyzed to evaluate the tissue motion in the subendocardium by a clinically accepted software [16]; results were further validated by ensuring that the longitudinal strain obtained by the 3D analysis was comparable (within a $\pm 5\%$ error range) to that obtained by 2D analysis.

The moving tissue surface was arranged in a 2D mesh defined by the 3D coordinates of material points $\mathbf{X}(s, \theta, t)$ set regularly at the beginning of contraction at time $t = 0$, whose parametric coordinates (s, θ) range from base to apex and circumferentially, respectively. The symmetric 2×2 strain-rate tensor is defined by

$$SR_{ij}(s, \theta, t) = \frac{1}{2h_j} \frac{\partial \mathbf{V}}{\partial x_j} \cdot \mathcal{T}_i + \frac{1}{2h_i} \frac{\partial \mathbf{V}}{\partial x_i} \cdot \mathcal{T}_j, \quad (1)$$

where the indices i and j take the value s or θ , $\mathbf{V}(s, \theta, t) = \frac{\partial \mathbf{X}}{\partial t}$ is the velocity vector of material points, $h_s(s, \theta, t)$ and $h_\theta(s, \theta, t)$ are the coordinate metric functions, and $\mathcal{T}_s(s, \theta, t)$ and $\mathcal{T}_\theta(s, \theta, t)$ are the unit tangent vectors. The strain tensor is then obtained by time integration of the strain-rate

$$St_{ij}(s, \theta, t) = \int_0^t SR_{ij} dt, \quad (2)$$

where $t = 0$ is taken at the beginning of contraction, and the end-systolic strain tensor is the eventual strain at the end of contraction. The strain tensor \mathbf{St} is transformed into a diagonal tensor where the two real eigenvalues represent the principal and secondary strain values, and the eigenvectors give the corresponding directions. Thus, tissue deformation, that in original coordinates presents longitudinal and circumferential contraction plus a shear deformation, corresponds to a pure strain deformation along the local eigendirections and no shear. Strain lines are then defined as the lines on the LV surface everywhere tangent to the principal eigenvector.

The LV strain curves are shown in Fig. 2 for the 15 normal individuals (a), (b) and the 15 athletes (c), (d). Principal strain decreases during fibers shortening up to a minimum value (about -30%) at the end of the contraction, and recovers during the biphasic LV dilatation up to zero deformation at the beginning of the following heartbeat. The secondary strain presents much smaller end-systolic values and occasionally even a slight dilatation during the contraction. Results are remarkably similar in the two groups, more compact in the second group that

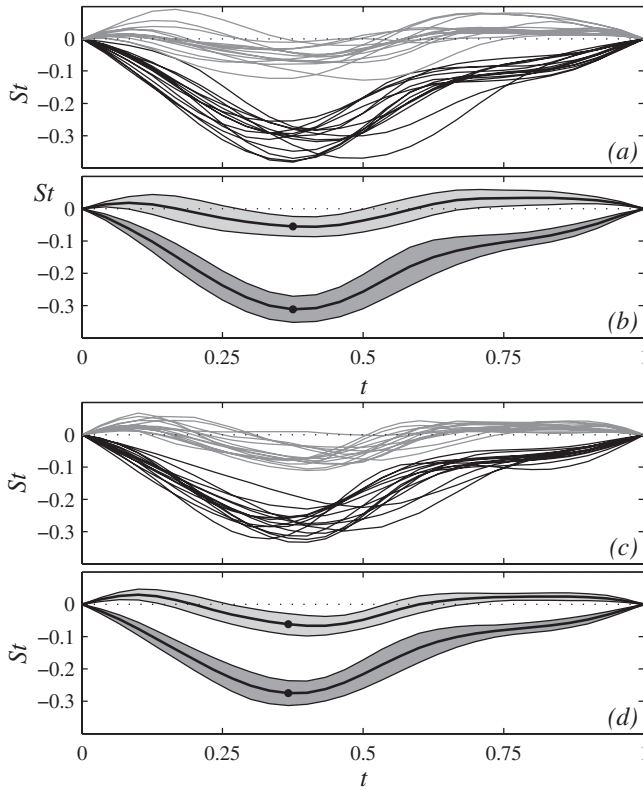


FIG. 2. Time evolution of the spatially averaged principal strain during a heartbeat computed *in vivo* for 15 normal subjects (a), (b), and for 15 athletes (c), (d). Panels (a) and (c) report the individual principal strain (black lines) and secondary strain (gray) curves; panels (b) and (d) show the corresponding average curves and standard deviation.

contains more homogenous subjects. A slightly lower value of strain is found in the athletes, a finding that is in agreement with previous reports for athletes at rest [17]. These results evidence the anisotropic character of contraction that is high along the principal direction and much lower transversal to it. Such a marked difference between principal and secondary strain suggests that the contraction is fundamentally driven along one-dimensional paths with little transversal connectivity. This, however, does not necessarily mean that the principal direction is along the anatomical direction of fibers; for example, the presence of two layers of crossing fibers differently directed (see Fig. 1) would produce a principal stress in an intermediate direction. The present results mean that contraction occurs predominantly along functional one-dimensional principal lines. These lines are certainly related by the fibers' direction but do not necessarily coincide with them because fibers have different layers, are linked transversally, and activate with different timings.

The pattern of the principal strain lines averaged over the uniform set of the 15 normal individuals and over the set of 15 athletes is shown in Fig. 3. It is reported separately for the two groups to emphasize the remarkable similarity between the two results, from *in vivo* sets acquired and

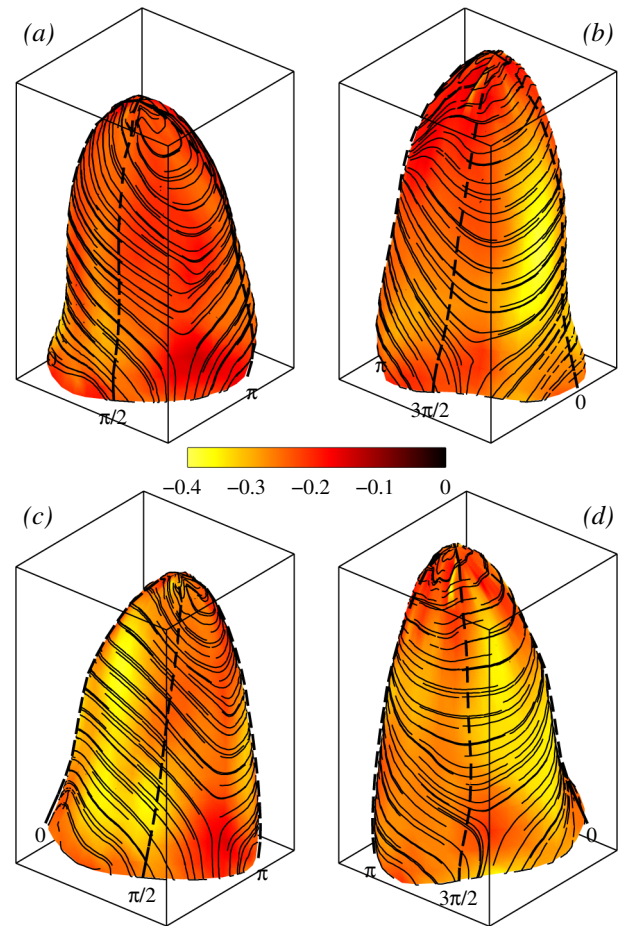


FIG. 3 (color online). Principal strain distribution and strain lines, at the end of a contraction, resulting from an average of 15 normal individuals (a) and (b), from two perspectives, and from 15 athletes (c) and (d). The LV is reported upside-down for visualization purpose. For anatomical reference, the value $\theta = 0$ corresponds to the position of the aortic outflow, and the right ventricle extends from there to about $\theta = \pi/2$.

processed by different clinical units. The strain-line pattern on the apical half of the LV matches the hypothesized pattern of myocardial fibers, which wraps around the apex on the anterior-lateral wall ($\frac{3}{2}\pi < \theta < 2\pi$) and converges toward the base at the inferior wall ($\frac{\pi}{2} < \theta < \pi$) where the ascending and descending bundles are expected to cross. On the basal half of the LV the anatomy is less explicit due to the presence of inhomogeneous valvular elements and circumferential wrapping of the muscular band [6,7,9]. Nevertheless, in both groups strain lines present a common behavior, connecting to the base before the aorta ($\theta < 0$) and after the end of the junction with the right ventricle ($\theta > \frac{\pi}{2}$).

The results reported must be taken with care as they are preliminary and present several limitations. The calculation does not include the entire 3D myocardium structure and is limited to its inner layer. The 3D echocardiography technology has a reduced spatial and temporal resolution

in comparison with 2D echocardiography although it gives theoretically a more complete picture of tissue deformation. The spatial resolution of the mesh is here made of 16 longitudinal \times 32 circumferential points, and it was verified that a higher resolution does not reveal any finer detail. Finally, the tissue tracking technique [16] is subjected to lack of accuracy in regions with poor image quality although care has been taken to validate the results and check reproducibility. On the other hand, all the subjects were selected for their excellent quality of echocardiographic recording, data are employed in integral or average sense only, and the cross agreement between individual results suggests that inaccuracies, unavoidable for *in vivo* studies, are presumably limited. The validity of data obtained from studies with poorer image quality remains unknown.

The analysis of the LV deformation in terms of principal strain demonstrates that contraction is dominated by one-dimensional strain along the principal direction while the transversal strain is much smaller. The principal strain thus reflects an effective measure of tissue contractility; moreover, the peculiar small contribution of transversal strain suggests that it may represent a sensible indicator of anomalous contractile behavior even at the early stage of a disease. In fact, the small transversal activity, presumably passive, is unable to counteract a starting irregularity in tissue behavior and may evidence such changes first. The spatial distribution of strain lines reflects the pattern of LV contraction; it represents the functional structure corresponding to the underlying anatomical architecture. Despite the complexity of the methodological chain, results appeared rather robust and reproducible among normal individuals. It can thus be expected that the presence of a disease, including localized regional dysfunctions, alters the strain-line pattern and can allow an identification of specific pathologies.

These preliminary interdisciplinary results of a novel methodology come from a multicenter study, which permitted a cross validation of methods and findings. They are remarkable enough to represent an initial physics-based reference for potential future medical applications. This study wants to indicate how this approach may represent an appropriate basis in the study of anisotropic materials and, in particular, biological tissues where the presence of fibers gives rise to anatomical preferable direction that may reflect functional lines.

Authors acknowledge Rolf Baumann (TomTec GmbH, Germany) for providing a modified version of their 3D tissue tracking software [16], which exports the raw data to be used for the principal strain analysis.

-
- [1] S.P. Timoshenko, *Theory of Elasticity* (McGraw-Hill Book Co., New York, 1934).
 - [2] B.D. Agarwal, L.J. Broutman, and K. Chandrashekara, *Analysis and Performance of Fiber Composites* (John Wiley & Sons, Hoboken, NJ, 2006).
 - [3] G.C. Engelmayr Jr., M. Cheng, C.J. Bettinger, J.T. Borenstein, R. Langer, and L.E. Freed, *Nature Mater.* **7**, 1003 (2008).
 - [4] S. Setayeshgar and A.J. Bernoff, *Phys. Rev. Lett.* **88**, 028101 (2001).
 - [5] G.D. Buckberg, *J. Thorac. Cardiovasc. Surg.* **124**, 863 (2002).
 - [6] F. Torrent-Guaspa, M.J. Kocica, A.F. Corno, M. Komeda, F. Carreras-Costa, A. Flotats, J. Cosin-Aguillar, and H. Wen, *Eur. J. Cardiothorac. Surg.* **27**, 191 (2005).
 - [7] H. Lombaert, J. Peyrat, P. Croisille, S. Rapacchi, L. Fanton, F. Cheriet, P. Clarysse, I. Magnin, H. Delingette, and N. Ayache, *IEEE Trans. Med. Imaging* **31**, 1436 (2012).
 - [8] P.P. Sengupta, J. Korinek, M. Belohlavek, J. Narula, M.A. Vannan, A. Jahangir, and B.K. Khandheria, *J. Am. Coll. Cardiol.* **48**, 1988 (2006).
 - [9] G. Buckberg, J.I.E. Hoffman, A. Mahajan, S. Saleh, and C. Coghlan, *Circulation* **118**, 2571 (2008).
 - [10] C.C. Moore, C.H. Lugo-Olivieri, E.R. McVeigh, and E.A. Zerhouni, *Radiology* **214**, 453 (2000).
 - [11] X. Zhong, B.S. Spottiswoode, C.H. Meyer, C.M. Kramer, and F.H. Epstein, *Magn. Reson. Med.* **64**, 1089 (2010).
 - [12] A. Nasiraei-Moghaddam and M. Gharib, *Am. J. Physiol. Heart Circ. Physiol.* **296**, H127 (2009).
 - [13] Y. Richter and E.R. Edelman, *Circulation* **113**, 2679 (2006).
 - [14] J. Narula, M.A. Vannan, and A.N. De Maria, *J. Am. Coll. Cardiol.* **49**, 917 (2007).
 - [15] G. Pedrizzetti and F. Domenichini, *Phys. Rev. Lett.* **95**, 108101 (2005).
 - [16] 4D LV-ANALYSIS 3.0, TomTec Imaging System GmbH, Unterschleissheim, Germany.
 - [17] L. Stefani, L. Toncelli, V. Di Tante, M.C.R. Vono, A. Moretti, B. Cappelli, G. Pedrizzetti, and G. Galanti, *Cardiovascular Ultrasound* **6**, 14 (2008).